Complementary Logic Implementation for Antiferromagnet Field-Effect Transistors

Chenyun Pan, Member, IEEE, and Azad Naeemi, Senior Member, IEEE

Abstract—In this paper, a compact and complementary logic implementation is proposed for antiferromagnet field-effect transistor (AFMFET) devices. The implementation enables a complete set of Boolean operations based on complementary logic as well as majority-gate logic. The impacts of several key devicelevel design parameters are investigated, such as the channel resistance and critical switching voltage, and their optimal values that minimize the overall energy-delay product (EDP) of a 32-bit arithmetic logic unit are quantified. In addition, it is shown that one can potentially take advantage of the large domain size of some AFM materials such as Chromia and build a compact majoritygate-based logic. The potential performance benefits of the majority-gate-based logic are also quantified. Compared to the conventional CMOS logic circuit, the one with AFMFET devices using majority-gates can potentially achieve 10× improvement in terms of the EDP.

Index Terms—Antiferromagnet FET, complementary logic, majority-gate logic, performance analysis.

I. INTRODUCTION

THERE is a global search for beyond-CMOS logic devices that can complement or even replace CMOS technology to alleviate the scaling challenges and sustain the exponential growth in chip throughput [1-4]. Magnetic devices have been at the center of this search as they provide new features, such as non-volatility and low-voltage operation [5, 6]. One set of the spintronic devices are current-driven, and some of the well-studied device concepts in this category include all-spin logic, charge-coupled spin logic, and domain wall logic devices [7-9]. However, the high current densities in current-driven devices increase the power dissipation, cause reliability issues, and lead to large static power dissipation.

To improve the computing energy-efficiency, voltage-controlled spintronic devices have been proposed. Some promising candidates include magnetoelectric magnetic tunneling junction devices, spin wave device, and composite-input magnetoelectric-based logic technology [10-12]. From a recent beyond-CMOS device benchmarking research, voltage-controlled spintronic devices are expected to dissipate orders of

Manuscript received August 21, 2018. This work was supported by the Semiconductor Research Corporation (SRC) nCORE Task 2760.003.

C. Pan is with the department of electrical engineering and computer science, the University of Kansas, Lawrence, KS 66045 USA. A. Naeemi is with the School of Electrical and Computer Engineering, Georgia Institute of Technology, Atlanta, GA 30332 USA. (e-mail: chenyun.pan@ku.edu).

magnitude less energy per binary switching operation compared to current-controlled magnetic devices [13]. However, most magnetic device concepts proposed so far are based on the switching of the magnetization of ferromagnets. The ferromagnet switching time is in the order of nanoseconds [14, 15], which is orders of magnitude slower compared to the conventional charge-based FETs. This large switching delay also leads to increased energy dissipation due to the leakage power in the readout circuitry [7-9].

To further improve the performance in terms of the switching speed, a recent study proposed an antiferromagnet field-effect transistor (AFMFET) device [16] whose schematic is shown in Fig. 1. By applying an input voltage on the gate, the magnetic order of the AFM layer is switched by the generated electrical field. The uncompensated surface magnetization of the AFM is tied to the magnetic order, and polarizes the spins of carriers in the spin-orbital coupling (SOC) channel and induces a preferred direction for conduction, i.e. either from source to drain or drain to source. This way, the polarity of the voltage applied to the gate determines which way current flows more easily. This operational characteristic differs significantly from the traditional spintronic devices that require the switching of a ferromagnet or movement of a ferromagnetic domain wall, whose switching speed is normally in the order of hundreds of picoseconds to nanoseconds [14, 17]. The switching speed of AFM layers has been reported to be at the sub-10ps range [16, 18], which is much faster and creates unique opportunities for fast and energy efficient logic implementations. Thanks to the low electrical field required to switch the AFM [19], the proposed device concept may potentially lead to energy efficient ultra-low voltage circuits. This non-volatile and voltage controlled device is expected to provide room temperature operation with ON/OFF ratios well beyond what can be achieved using magnetic tunnel junctions (MTJs) [16].

There are several experiments indicating that the magnetic order in Chromia can be switched back and forth via an applied electric field in the presence of a static magnetic field [20, 21]. The creation of a preferred direction via SOC has only been predicted based on first principle calculations and is yet to be confirmed experimentally [16]. While research on the experimental demonstration of the device is ongoing, it is helpful to evaluate the potential performance of the proposed device, determine whether or not a flexible and complete logic family can be implemented with this device, and identify the desired material and device level parameters to maximize the

overall circuit-level performance. The results can provide important motivation and guidance for device researchers and experimentalists working in this area.

Regarding the logic implementation, only a multiplexerbased logic has been proposed in the original proposal [16]. However, such logic lacks gain, and a more generic and robust logic implementation is needed for a wider range of applications. In this paper, a novel logic implementation is proposed for AFMFET devices to achieve complementary logic similar to what can be achieved in CMOS logic. However, to further increase density and improve energy and delay, a majority-gate based logic is proposed taking advantage of the large domain size in some antiferromagnetic materials such as Chromia. The proposed logic implementation does not need any dedicated MOSFETs to drive the next stage or special clocking scheme. It satisfies all five essential requirements for general logic applications, including nonlinearity, concatenability, feedback prevention, and a complete set of Boolean operations. The proposed logic implementation also has a compact layout that is comparable to the CMOS technology.

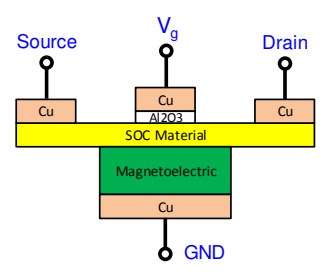


Fig. 1. Schematic of AFMFET device [16].

The rest of the paper is organized as follows. Section II proposes two logic implementations for AFMFET devices, including complementary and majority-gate logic gates. Section III describes the device-level performance modeling approach to estimate the intrinsic delay, energy, and footprint area of the proposed AFMFET logic. The circuit-level performance analyses and benchmarking results and discussions are presented in Section IV. Finally, conclusions are made in Section V.

II. PROPOSED LOGIC IMPLEMENTATION

To utilize the unique feature of the directionality of conduction present in AFMFET devices, we propose a complementary logic implementation. The top-down and 3D views of the proposed logic gate are shown in Fig. 2. For an inverter, the direction of the currents flowing through the SOC materials in the pull-up and pull-down networks are right-to-left and left-to-right, respectively. Depending on the input voltage, the boundary magnetization of the AFM layer switches, leading to an asymmetry of the current flow in the two SOC channels. For instance, when the input voltage is low as shown in Fig. 2 (a), the preferred current direction is from left-to-right. Therefore, the output voltage is pulled close to VDD, achieving the inversion operation. The voltage transfer

characteristic (VTC) of the inverter is illustrated in Fig. 3. The device is considered active and has a large gain when the input voltage is above or below half of the supply voltage by the threshold voltage of the AFM, V_{crit} .

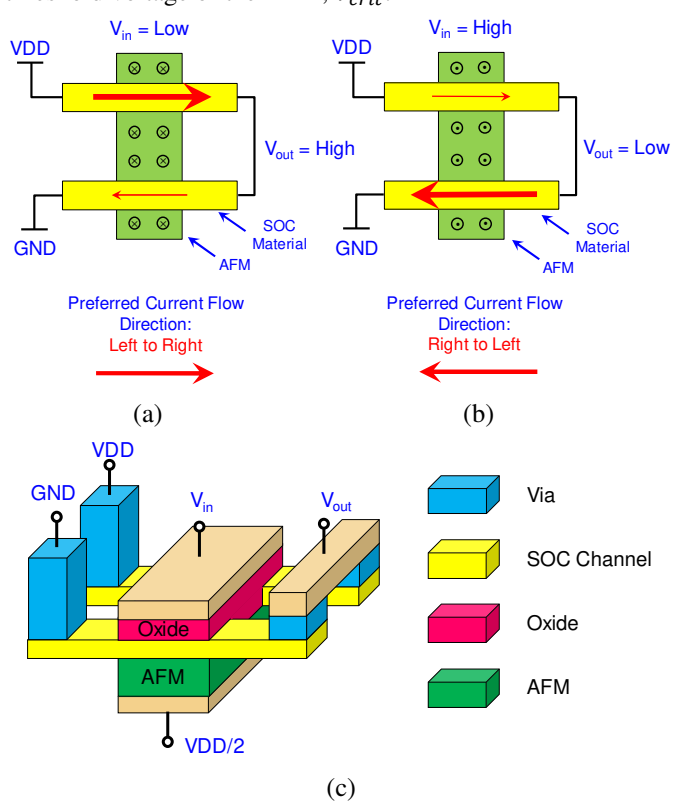


Fig. 2. (a) and (b) shows a top-down view for an AFMFET-based inverter when the input is GND and VDD, respectively. (c) shows the 3D structure view of the proposed AFMFET-based inverter implementation.

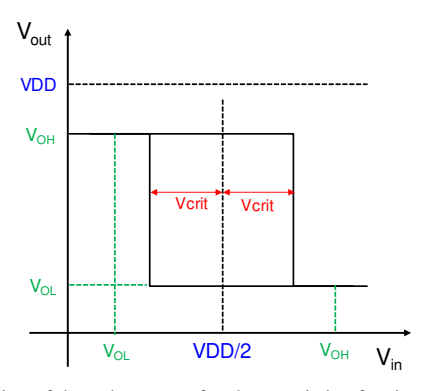


Fig. 3. Illustration of the voltage transfer characteristic of an inverter.

The same technique is applicable to all complementary logic gates, such as a NAND2 gate, shown in Fig. 4. When multiple current paths are connected in series/parallel, the overall current is dominated by the least/most conductive path. This is quite similar to what happens in CMOS logic, with the difference being that p- and n-channel devices are replaced with devices with left-to-right and right-to-left current paths, respectively. By connecting AFMFET devices in the pull-up and pull-down networks properly, all complementary logic functions can be achieved. The voltage generated at the output is static, which

can directly drive the input of the next stage without using auxiliary field-effect transistors or any special clocking schemes as needed in prior magnetoelectric-based device proposals [12].

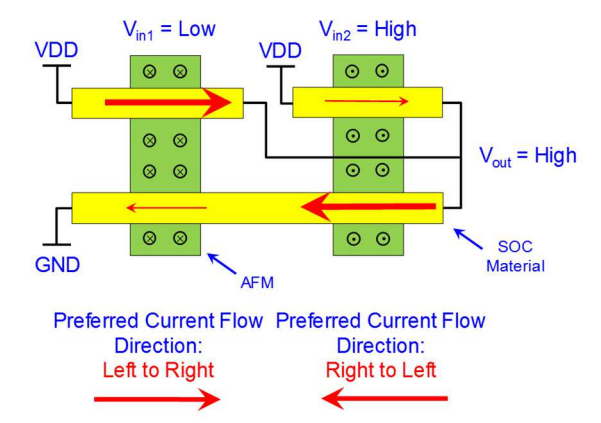


Fig. 4. Proposed AFMFET-based 2-input NAND logic implementation.

Another option to implement a complete logic set is by creating a majority gate. From experimental results in [22], the typical domain size in Chromia is about 5µm which is more than 10× larger compared to the AFM layer used in this paper. Therefore, a single-domain assumption is expected to be valid, and this property has been used in the past proposals to implement a majority gate based on MEMTJ device [12, 23]. In these proposals, three input gates are used and the surface magnetization of Chromia is controlled by the majority of the inputs. Here, we adopt the majority gate concept and incorporate it with the complementary AFMFET logic as shown in Fig. 5. Compared to the prior magnetoelectric majority logic gate proposals [12, 23] that use a dynamic logic style to implement Boolean logic, the proposed majority gate does not need a dedicated preset clocking and is more compatible with the CMOS static circuits and standard cell design.

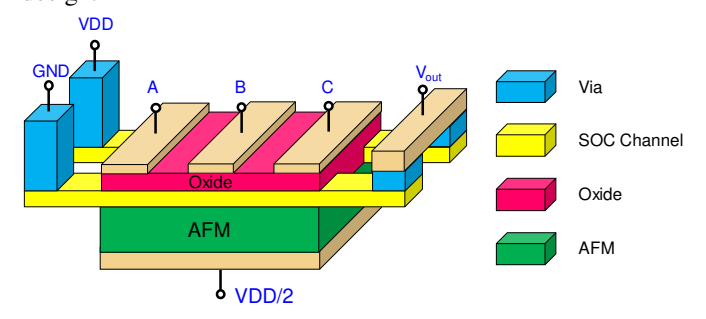


Fig. 5. 3D device structure view of a majority-gate using AFMFET devices.

III. MODELING APPROACH

In this section, the intrinsic delay and energy of the proposed logic gates are modeled to enable the circuit-level performance analysis in Section IV. Instead of using spin-transfer-torque (STT) as the switching mechanism, the AFMFET device relies on voltage controlled magnetoelectric (exchange bias) effect [24].

The intrinsic delay of an AFMFET logic gate is modeled as

$$t_{int} = t_{AFM} + t_{RC}, (1)$$

where t_{AFM} is the intrinsic switching delay of AFM, which is assumed to be 10 ps, and t_{RC} is the electrical RC delay based on the equivalent circuit model illustrated in Fig. 6, where R_{ν} and R_d are the pull-up and pull-down network resistances, respectively, C_{AFM} , C_{ox} , and C_q are the AFM capacitance, oxide capacitance, and quantum capacitance. The dielectric constants for AFM and oxide are 12 and 3.9 [25], respectively, and the thickness of AFM and oxide layers are 10 nm and 1 nm, respectively. The quantum capacitance is assumed to be 50% of the gate oxide capacitance. The values of the pull-up and pulldown resistances are determined by the SOC channel resistance, which depends on the direction of magnetoelectric polarization of the AFM. The relation between the current and gate voltage, shown in Fig. 7, is obtained by using Non-Equilibrium Green's Function (NEGF) transport simulations in a 2-D ribbon with a width of 20 nm and a band mass of $0.1m_e$ [16]. A conservative value of exchange splitting of 0.1 eV at 300 K is assumed.

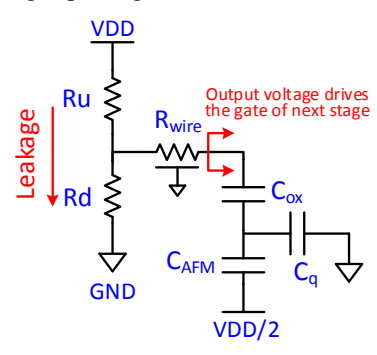


Fig. 6. Equivalent circuit model for AFMFET-based logic implementation.

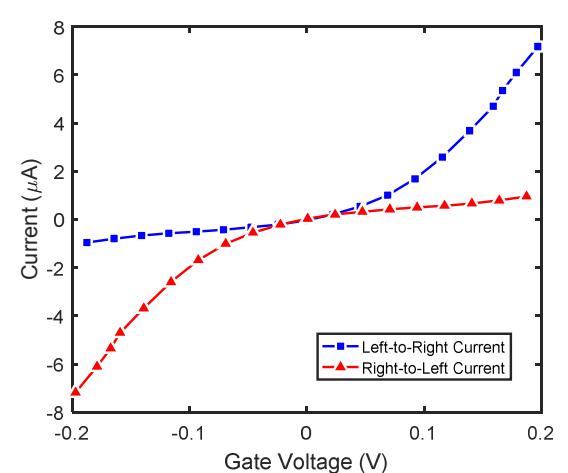


Fig. 7. IV Characteristics of the AFMFET device [16].

To model the energy dissipation of the AFMFET logic, the dynamic switching energy during charging and discharging the gate capacitance is written as

$$E_{dyn} = \frac{1}{2} C_g \Delta V^2, \tag{2}$$

where ΔV is the voltage swing at the output. To drive the next stage without additional transistors, the minimum value of ΔV is determined by the critical switching voltage of the AFM, V_{AFM} , which is written as $\Delta V = V_{AFM}(C_{AFM} + C_{ox})/C_{ox}$. Note that both the electric field, E, and a small symmetry breaking magnetic field, E, are needed simultaneously to perform isothermal switching of Chromia, where the product of E and E needs to overcome a critical threshold [19, 26]. In section E0, we will investigate the performance of AFMFETs with three E1, where E2 is the performance of AFMFETs with three E3.

For the leakage energy calculation, if the ON-OFF ratio is small, a supply clocking scheme can be employed such that the device only consumes leakage power during the logic operation [27]. The corresponding leakage energy is written as

$$E_{leak} = \frac{VDD^2}{R_u + R_d + R_{clk}} t_{clk},$$
 (3)

where t_{clk} is half of the clock period, R_{clk} is the equivalent ON resistance of the clocking transistor per AFMFET logic gate, and VDD is the supply voltage. For a given V_{AFM} , the voltage swing at the output can be calculated, which determines the supply voltage according to the equation below:

$$VDD = \frac{2\Delta V(R_u + R_d + R_{clk})}{|R_u - R_d|}.$$
 (4)

In this paper, the clock speed is limited to 5 GHz, and the transistor resistance follows the 15 nm CMOS high-performance device used in the previous benchmarking work [2], assuming the width of the transistor is 150 nm.

The switching energy associated with the supply clocking is written as

$$E_{clk} = \frac{1}{2} (C_{wire} + C_{clk}) VDD^2, \tag{5}$$

where C_{wire} and C_{clk} are the interconnect capacitance and gate capacitance of the clocking transistors. Interconnect parasitic capacitance is 0.15 fF/ μ m, which is estimated based on a validated capacitance model [28, 29], and the input capacitance of clocking transistors is 0.2 fF [2]. The number of logic gates shared by a clocking transistor is set as 10 to achieve the proper balance between footprint area, dynamic and leakage energy overheads of the supply clocking.

The total intrinsic energy of an AFMFET logic gate is the summation of all energy components:

$$E_{int} = E_{dyn} + E_{leak} + E_{clk}. (6)$$

Fig. 8 illustrate the layout of the proposed AFMFET logic using complementary and majority-gate based implementations. The design rule follows the previous benchmarking methodology [2, 13], where the minimum distance between two contacts is 4F. The footprint area of the proposed AFMFET logic is comparable to its CMOS counterpart for a basic inverter. For a two-input NAND gate, 33% of the footprint area overhead is observed. This is mainly due to the fact that to achieve opposite current flow directions in the pull-up or pull-down network, the source and drain of the

AFMFET devices cannot be shared. For a majority gate, the AFMFET device provides a large area saving thanks to the compact design and layout.

IV. PERFORMANCE ANALYSES

In this section, the circuit-level performance of the proposed AFMFET logic implementations is analyzed and benchmarked against various beyond-CMOS technologies. The benchmarking circuit is a 32-bit ALU, which is adapted from a

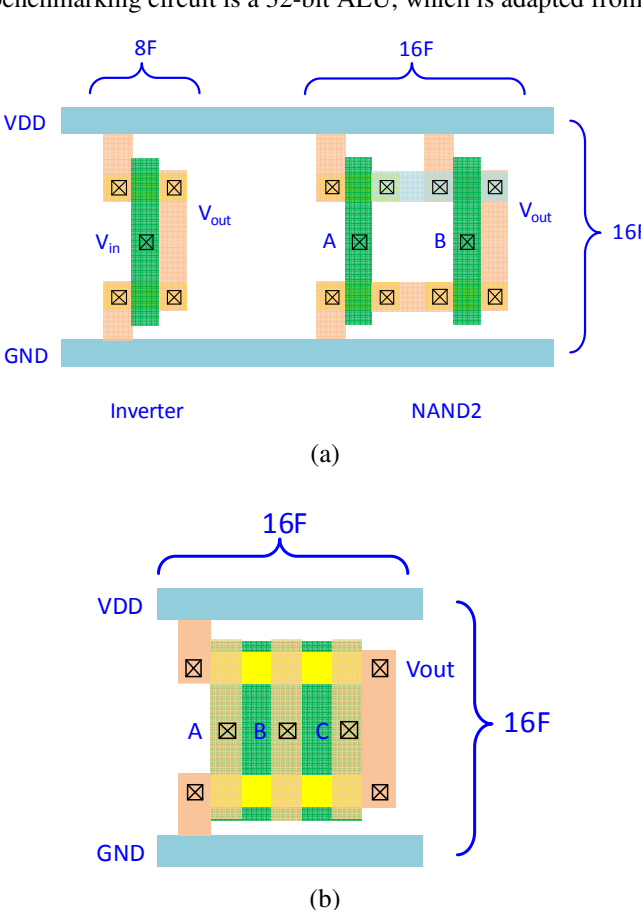


Fig. 8. Proposed layout views for an (a) inverter and 2-input NAND gate and (b) majority gate using AFMFET devices.

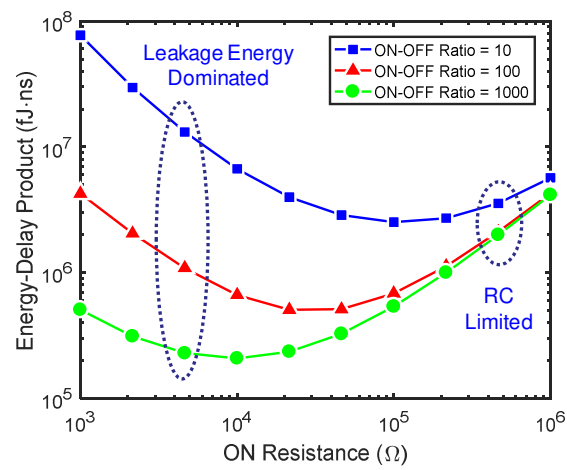


Fig. 9. Energy-delay product as a function of ON resistance of the AFMFET channel at different ON-OFF ratio assumptions.

uniform benchmarking tool [2]. Based on the modeling approach described in Section III, the delay, energy dissipation, and footprint area per logic gate are evaluated and used as the basic building block in the benchmarking tool.

A. Channel Resistance Optimization

To properly design and optimize the device and circuit performance, one key parameter investigated in this paper is the channel resistance. The choice of material and doping level for the channel can result in vastly different channel resistance values. Fig. 9 shows the energy-delay product (EDP) per ALU operation by sweeping the channel resistance at three hypothetical ON-OFF ratios under a given critical switching voltage of 100 mV. For a small channel resistance, the leakage energy dominates the overall energy dissipation because of the large current flowing from VDD to GND. As the channel resistance increases beyond a certain point, the delay keeps increasing due to the significantly larger RC delay values. The energy dissipation becomes dominated by the switching energy associated with charging and discharging the AFM. As a result, optimal channel resistances exist to minimize the overall EDP.

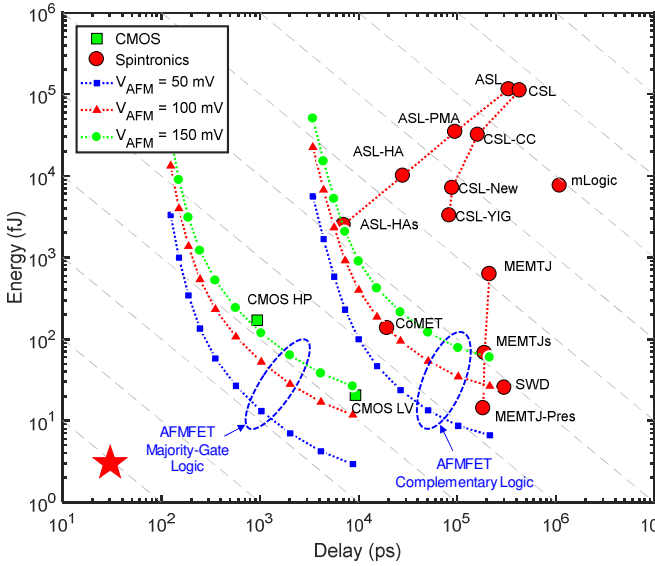
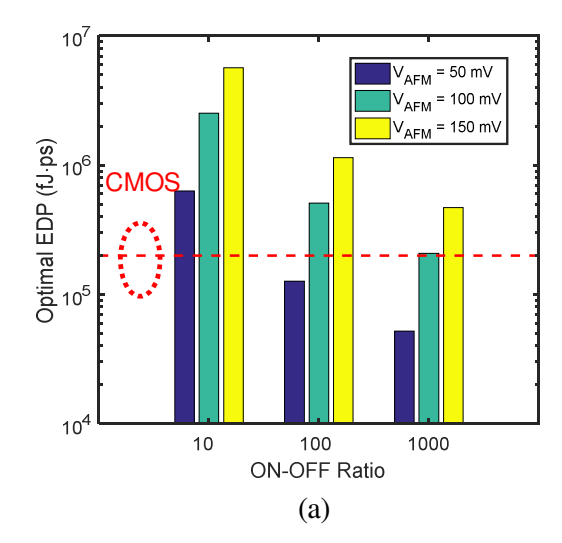


Fig. 10. Comparison of energy and delay of a 32-bit adder among various charge- and spin-based devices.

B. Circuit-Level Analysis and Benchmarking

To compare AFMFET devices with other spintronic devices and the conventional CMOS devices, we use a uniform benchmarking methodology with a 32-bit ALU as the benchmarking circuits [2]. The energy versus delay per ALU operation for AFMFET devices at three different critical switching voltages are shown in Fig. 10. Since the product of the applied electrical and magnetic fields needs to overcome a critical threshold [19, 26], a smaller supply voltage requires a larger static magnetic field. In this paper, three critical switching voltages of 50 mV, 100 mV, and 150 mV are considered. The corresponding and magnetic fields are 628 Oe, 314 Oe, and 214 Oe, respectively [19].

In general, spintronic devices are slower due to the limitation of the magnet switching delay. The voltage-controlled devices,



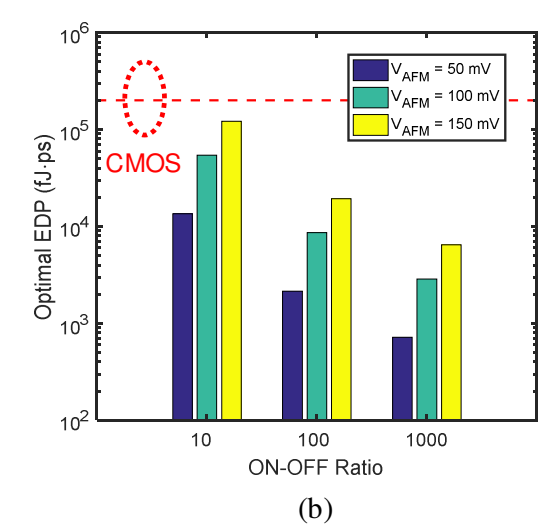


Fig. 11. Comparison of optimal EDP of a 32-bit adder using CMOS and AFMFET devices with (a) complementary and (b) majority-gate logic implementation.

including the spin wave device (SWD), composite-input magnetoelectric-based logic technology (CoMET), and magnetoelectric magnetic (MEMTJ) consume much less energy compared to the current-driven devices, such as the allspin logic (ASL) and charge-spin logic (CSL) devices. For the proposed AFMFET logic, both complementary and majoritygate-based implementations perform better compared to their spintronic counterparts. The main advantage is the fast switching time of the AFM without the need of switching an entire ferromagnet or moving a domain wall inside a ferromagnet. At the optimal channel resistance with a small critical switching voltage of 50 mV, the AFMFET with the complementary logic implementation provides an EDP comparable with its CMOS counterpart. However, the majoritygate-based AFMFET logic implementation can potentially provide up to 30× EDP reduction. This is because a variety of the logic functions can be implemented quite efficiently with majority-gates. For example, only one majority operation is needed to generate the carry out in a full adder. This reduces the number of logic gates in the critical path significantly and saves

the energy due to fewer logic gates required to achieve the same functionality.

The results shown in Fig. 10 are based on an ON-OFF ratio of 10 [16]. To quantify the benefits of the proposed AFMFET logic with an improved ON-OFF ratio, Fig. 11 shows the EDP of a 32-bit adder at various ON-OFF ratios up to 10³ with the optimal channel resistance. For both complementary and majority-gate logic implementations, the performance of AFMFET improves as the ON-OFF ratio increases. For a small AFM critical switching voltage of 50 mV with a relatively large ON-OFF ratio of 10³, the majority-gate-based AFMFET logic implementation can potentially reduce the EDP by two orders of magnitude compared to the CMOS counterparts. The main advantage comes from the ultra-low operation voltage as well as the fast AFM switching delay. In addition, the majority-gate based logic is more efficient compared to its complementary logic implementation.

V. CONCLUSION

This paper proposes two novel logic implementations for AFMFET devices with complementary logic and majority-gate logic. The proposed logic gates satisfy five essential properties, allowing AFMFETs to be used as fast and energy-efficient stand-alone logic devices. Optimal channel resistance is found to minimize the overall EDP under different critical switching voltages and ON-OFF ratios. At the circuit-level analysis, AFMFET devices based on majority-gate implementations are projected to be more energy efficient compared to their CMOS counterparts thanks to their low operating voltages and the need for fewer devices needed for implementing adders.

REFERENCES

- [1] K. J. Kuhn, "CMOS scaling for the 22nm node and beyond: Device physics and technology," in VLSI Technology, Systems and Applications (VLSI-TSA), 2011 International Symposium on, 2011, pp. 1-2.
- [2] D. E. Nikonov and I. A. Young, "Benchmarking of beyond-CMOS exploratory devices for logic integrated circuits," *Exploratory Solid-State Computational Devices and Circuits, IEEE Journal on*, vol. 1, pp. 3-11, 2015
- [3] M. T. Bohr and I. A. Young, "CMOS Scaling Trends and Beyond," *IEEE Micro*, vol. 37, pp. 20-29, 2017.
- [4] J.-P. Wang, S. S. Sapatnekar, C. H. Kim, P. Crowell, S. Koester, S. Datta, et al., "A pathway to enable exponential scaling for the beyond-cmos era," in *Proceedings of the 54th Annual Design Automation Conference 2017*, 2017, p. 16.
- [5] S. A. Wolf, J. Lu, M. R. Stan, E. Chen, and D. M. Treger, "The promise of nanomagnetics and spintronics for future logic and universal memory," *Proceedings of the IEEE*, vol. 98, pp. 2155-2168, 2010.
- [6] S. Manipatruni, D. E. Nikonov, and I. A. Young, "Beyond CMOS computing with spin and polarization," *Nature Physics*, vol. 14, p. 338, 2018
- [7] B. Behin-Aein, D. Datta, S. Salahuddin, and S. Datta, "Proposal for an all-spin logic device with built-in memory," *Nature Nanotechnology*, vol. 5, pp. 266-270, 2010.
- [8] D. Morris, D. Bromberg, J.-G. J. Zhu, and L. Pileggi, "mLogic: Ultra-low voltage non-volatile logic circuits using STT-MTJ devices," in Proceedings of the 49th Annual Design Automation Conference, 2012, pp. 486-491.
- [9] S. Datta, S. Salahuddin, and B. Behin-Aein, "Non-volatile spin switch for Boolean and non-Boolean logic," *Applied Physics Letters*, vol. 101, p. 252411, 2012.
- [10] M. G. Mankalale, Z. Liang, Z. Zhao, C. H. Kim, J.-P. Wang, and S. S. Sapatnekar, "CoMET: Composite-input magnetoelectric-based logic

- technology," Exploratory Solid-State Computational Devices and Circuits, IEEE Journal on, vol. 3, pp. 27-36, 2017.
- [11] S. Dutta, D. E. Nikonov, S. Manipatruni, I. A. Young, and A. Naeemi, "Phase-dependent deterministic switching of magnetoelectric spin wave detector in the presence of thermal noise via compensation of demagnetization," *Applied Physics Letters*, vol. 107, p. 192404, 2015.
- [12] N. Sharma, A. Marshall, J. Bird, and P. Dowben, "Magneto-electric magnetic tunnel junction logic devices," in *Energy Efficient Electronic* Systems (E3S), 2015 Fourth Berkeley Symposium on, 2015, pp. 1-3.
- [13] C. Pan and A. Naeemi, "An Expanded Benchmarking of Beyond-CMOS Devices Based on Boolean and Neuromorphic Representative Circuits," *IEEE Journal on Exploratory Solid-State Computational Devices and Circuits*, vol. 3, pp. 101-110, 2017.
- [14] M. Cubukcu, O. Boulle, N. Mikuszeit, C. Hamelin, T. Brächer, N. Lamard, et al., "Ultra-Fast Perpendicular Spin-Orbit Torque MRAM," IEEE Transactions on Magnetics, vol. 54, pp. 1-4, 2018.
- [15] G. E. Rowlands, S. V. Aradhya, S. Shi, E. H. Yandel, J. Oh, D. C. Ralph, et al., "Nanosecond magnetization dynamics during spin Hall switching of in-plane magnetic tunnel junctions," *Applied Physics Letters*, vol. 110, p. 122402, 2017.
- [16] P. A. Dowben, C. Binek, K. Zhang, L. Wang, W.-N. Mei, J. P. Bird, et al., "Towards a strong spin-orbit coupling magneto-electric transistor," IEEE Journal on Exploratory Solid-State Computational Devices and Circuits, 2018.
- [17] S. V. Aradhya, G. E. Rowlands, J. Oh, D. C. Ralph, and R. A. Buhrman, "Nanosecond-timescale low energy switching of in-plane magnetic tunnel junctions through dynamic oersted-field-assisted spin Hall effect," *Nano letters*, vol. 16, pp. 5987-5992, 2016.
- [18] T. Satoh, B. B. Van Aken, N. P. Duong, T. Lottermoser, and M. Fiebig, "Ultrafast spin and lattice dynamics in antiferromagnetic Cr 2 O 3," *Physical Review B*, vol. 75, p. 155406, 2007.
- [19] X. He, Y. Wang, N. Wu, A. N. Caruso, E. Vescovo, K. D. Belashchenko, et al., "Robust isothermal electric control of exchange bias at room temperature," *Nature materials*, vol. 9, p. 579, 2010.
- [20] T. Kosub, M. Kopte, R. Hühne, P. Appel, B. Shields, P. Maletinsky, et al., "Purely antiferromagnetic magnetoelectric random access memory," Nature communications, vol. 8, p. 13985, 2017.
- [21] K. Toyoki, Y. Shiratsuchi, A. Kobane, C. Mitsumata, Y. Kotani, T. Nakamura, et al., "Magnetoelectric switching of perpendicular exchange bias in Pt/Co/α-Cr2O3/Pt stacked films," Applied Physics Letters, vol. 106, p. 162404, 2015.
- [22] N. Wu, X. He, A. L. Wysocki, U. Lanke, T. Komesu, K. D. Belashchenko, et al., "Imaging and control of surface magnetization domains in a magnetoelectric antiferromagnet," *Physical review letters*, vol. 106, p. 087202, 2011.
- [23] C. Pan, S. Dutta, and A. Naeemi, "Magnetoelectric Computational Devices," ed: Google Patents, 2018.
- [24] W. Kleemann, "Magnetoelectric spintronics," *Journal of Applied Physics*, vol. 114, p. 027013, 2013.
- [25] H. Scherer, T. Weimann, P. Hinze, B. Samwer, A. Zorin, and J. Niemeyer, "Characterization of All-Chromium Tunnel Junctions and Single Electron Tunneling Devices Fabricated by Direct-Writing Multilayer Technique," arXiv preprint cond-mat/9907078, 1999.
- [26] S. Mu, A. L. Wysocki, and K. D. Belashchenko, "First-principles microscopic model of exchange-driven magnetoelectric response with application to Cr 2 O 3," *Physical Review B*, vol. 89, p. 174413, 2014.
- [27] V. Calayir, D. E. Nikonov, S. Manipatruni, and I. A. Young, "Static and clocked spintronic circuit design and simulation with performance analysis relative to CMOS," *IEEE Transactions on Circuits and Systems I: Regular Papers*, vol. 61, pp. 393-406, 2014.
- [28] J.-H. Chern, J. Huang, L. Arledge, P.-C. Li, and P. Yang, "Multilevel metal capacitance models for CAD design synthesis systems," *Electron Device Letters*, *IEEE*, vol. 13, pp. 32-34, 1992.
- [29] C. Pan, R. Baert, I. Ciofi, Z. Tokei, and A. Naeemi, "System-Level Variation Analysis for Interconnection Networks at Sub-10-nm Technology Nodes Using Multiple Patterning Techniques," *Electron Devices, IEEE Transactions on*, vol. 62, pp. 2071-2077, 2015.